scientific reports

Check for updates

OPEN

Hippocampal-prefrontal functional neural networks in a rat model of fragile X syndrome are poorly organized with limited resiliency

Mohamed Ouardouz[1], Patrick Jasinski[1], Mohamed Khalife[1,3], J. Matthew Mahoney[2], Amanda E. Hernan[1,3] & Rod C. Scott[1,3,4,5]✉

Fragile X Syndrome (FXS) is a common cause of autism spectrum symptoms. The genetic mutation results in multiple molecular alterations that are hypothesized to negatively impact neural circuit development although the nature of any functional neural dynamic consequences remain unclear. Therefore, the characteristics of hippocampal-prefrontal (H-PFC) network dysfunction were investigated in a rat model of FXS. FMR-KO and control rats underwent behavioral tests assessing sociability, memory, and anxiety to validate and replicate previously recognized deficits. Single-unit electrophysiology in the H-PFC circuit during exploration was used to measure patterns of action potential firing that were then compared between groups using generalized linear mixed models. FMR-KO rats demonstrated significant behavioral deficits in sociability, spatial learning, and anxiety. These rats also exhibited abnormal firing patterns outside of times when specific behavioral tasks were being performed. The network firing is less precise, more fragmented and with poor H-PFC communication in FXS. These findings suggest that disruptions in 'exploration' neural network dynamics impair the ability of networks to be appropriately engaged during specific behavioral tasks, leading to the observed deficits in social behavior, memory, and anxiety.

Keywords Fragile X syndrome, Autism spectrum disorder, Neural dynamics, Animal behavior, Systems neuroscience

Fragile X Syndrome (FXS) is a common monogenic cause of autism spectrum disorder (ASD)[1,2] often associated with learning, cognitive and behavioral concerns. Characterization of pathophysiological mechanisms responsible for the phenotype could identify novel therapeutic targets. To date, extensive evaluation at the cell biology level[3–5] has not resulted in markedly effective therapies. We therefore shift focus to neural network dynamics, specifically action potential firing patterns, as abnormal firing patterns could ultimately represent a therapeutic target for affected people who desire an improvement in symptoms. The ASD phenotype in FXS implicates hippocampal-prefrontal cortex (H-PFC) neural circuit dysfunction[6–8] and therefore we evaluated H-PFC dynamics during exploration in an open field, in a rat model of FXS.

There are several studies in humans with ASD that have shown that the hippocampus and the PFC are abnormal. The hippocampus of people with ASD can show histological abnormalities including increased neural density, abnormal interneuron numbers[9] and abnormalities of dendritic branching[10], consistent with that seen in the FMR-KO rat. The hippocampi also reveal changes in volume with both increases and decreases compared to controls[6,11], decreased blood flow and metabolic aberrations[6]. The prefrontal cortex may be larger in people with autism, and this may be associated with reduced activation as shown by fMRI in humans[12] and PET studies in the valproic acid animal model[13]. The H-PFC circuit is also important for regulation of anxiety[14]. These abnormalities have been implicated in the pathogenesis of the memory, language, anxiety, social and learning impairments frequently seen in people with ASD and support the view that the H-PFC circuit is abnormal in people with ASD. This justifies our choice of evaluating this specific neural network.

[1]Nemours Children's Hospital, 1600 Rockland Road, Wilmington, DE 19803, USA. [2]The Jackson Laboratory, 600 Main Street, Bar Harbor, ME 04609, USA. [3]University of Delaware, 210 South College Street, Newark, DE 19716, USA. [4]Sidney Kimmel College of Medicine, Thomas Jefferson University, 1035 Walnut Street, Philadelphia, PA 19107, USA. [5]Great Ormond Street Hospital NHS Trust, Great Ormond Street, London WC1N 3JH, UK. ✉email: rodney.scott@nemours.org

FXS results from a mutation in which a DNA segment, known as the CGG triplet repeat, is expanded within the *FMR1* gene. The expanded CGG triplets lead to decreased expression of the *FMR1* gene with consequent absence of the FMR1 protein[15–17]. This impacts the nuclear export[15,18,19], cytoplasmic transport and translational control of > 1000 mRNAs that regulate protein synthesis, thereby modifying synaptogenesis, maturation of dendritic spines, cell–cell communication, cytoskeletal and microtubular structure, and metabolic regulators[19–28]. These abnormal processes disrupt normal maturation and structure of neural networks[29–31] that could result in the emergence of abnormal neural network dynamics.

We reproduce abnormal behaviors[32] across several domains in the FMR-KO rat and define disrupted neural network dynamics during non-specific exploratory behavior. We suggest that the abnormally functioning 'exploration' network is unable to be appropriately engaged during a range of H-PFC dependent tasks thereby leading to the observed abnormal cognitive function.

Results

The results are reported according to ARRIVE guidelines. We initially carried out behavioral tests to characterize social, memory and anxiety phenotypes in adult FMR-KO rats. These data were collected across several cohorts. The initial cohorts carried out the tasks in the following order (Barnes Maze [day 1–6], Social interaction [Day 9] and light–dark box [Day 11–13]). Not all the animals completed all the tasks and those that did not actively participate were excluded. To ensure sufficient sample sizes for each task the latter cohorts were tested in the order: Social interaction, Barnes maze and then light dark box.

FMR-KO rats display sociability deficits

A 3-chamber sociability task was performed in 11 FMR-KO rats and 9 controls. In session 1 the animals were exposed to a novel rat and an inanimate object. Normal rats prefer interacting with the rat rather than the object (Fig. 1A). A discrimination index of 1 represents the situation in which all the interaction was with the novel rat, and a value of − 1 represents all the interaction being with the object. Control rats have a mean discrimination index of 0.73 ± 0.09 (mean ± 1 s.e.) and FMR-KO rats have a mean discrimination index of 0.36 ± 0.09 (Wald Chi-Square = 5.85, $p = 0.01$). In session 2 the animals were exposed to the same rat as in session 1, or a novel rat. Neither the controls nor the FMR-KO rats showed a preference for the novel rat over the familiar rat ($p > 0.05$ for both groups).

FMR-KO rats learn a spatial task less effectively

The Barnes maze task was carried out by 18 rats (10 FMR-KO and 8 controls) (Fig. 1B). After one day of habituation, the rats had five days to learn to find a hidden escape hole using distal spatial cues defined as a spatial strategy. A serial strategy is defined as one in which the animals visit each hole sequentially until the appropriate hole is found; this strategy is not hippocampal-dependent and usually indicates a deficit in hippocampal spatial cognition. A random strategy is defined as one in which the animal randomly visits holes until the escape is identified. The time it takes for the rat to escape, and how that time changes over sessions, was evaluated. There is a main effect of day (F = 4.4, df1 = 4, df2 = 76; $p = 0.006$) suggesting that both groups of animals improved with increasing exposure to the environment. The mean latency to escape, across both groups, on day 1 was 40.4 ± 4.2 s. The latency decreased to 18.1 ± 3.7 s on day 5. There is no main effect of group, averaged over days. FMR-KO animals had a mean latency to escape, averaged over 5 days of 27.6 ± 2.4 s, and the controls had a mean latency of 26.9 ± 2.7 s ($p = 0.84$). However, there is a difference in the trajectory of learning over time as evidenced by a significant day*group interaction (F = 2.9, df1 = 4, df2 = 76; $p = 0.028$). Pairwise analyses in the control rats showed a systematic decrease in latency from day 1 and day 2 to day 5 with significant differences between those days. The FMR-KO rats had a significant reduction in latency between day 1 and day 2, but no subsequent significant reduction in latency.

We further evaluated the Barnes maze behavior to evaluate the strategies used for solving the maze. Each trial was categorized as spatial (the animal moves straight to the escape), serial (the animal goes from hole to hole until they find the escape) or random (the animal just tries holes until they find the escape). We used a multinomial generalized linear mixed model to evaluate whether the proportion of trials of each type differed as a function of group and day. We show a main effect of group (F = 97.9, df1 = 2, df2 = 225; $p < 0.001$) and day (F = 100.8, df1 = 8, df2 = 225; $p < 0.001$), and a significant group*day interaction (F = 95.6, df1 = 8, df2 = 225; $p < 0.001$). The FMR-KO rats are more likely to take a serial approach (not seen in the controls) or a random approach whereas the controls display an increasing spatial strategy over time See Fig. 1B). Thus, even though there is no main effect of group when evaluating latency to finding the escape, the strategies for achieving the latency are very different, with the expected spatial strategy being used more commonly in control animals. Thus, control animals showed progressive spatial learning that was not observed in the FMR-KO rats supporting the view that the FMR-KO rats have a deficit in spatial cognition.

FMR-KO rats are anxious

Anxiety was evaluated in 13 rats (5 controls, 8 FMR-KO) using a light/dark box[33,34], a task based on the innate aversion of rats to brightly illuminated open areas (Fig. 1C). Alternative tests like the elevated plus maze test spatial anxiety and were not pursued in this study given that we wanted to evaluate a breadth of behavior, rather than have several tests evaluating a single behavior. The data were analyzed in two complementary ways. First, we evaluated the amount of time that the animals spent in the lighted area. Controls spent a median of 243 s (IQR; 146–268 s) compared to a median of 123 s (IQR; 38–159 s) in FMR-KO rats (Wald Chi-Square – 5.3; $p = 0.03$). We then evaluated the proportion of attempts to enter the lighted area that resulted in going into that area. Control rats entered the lighted area on 58% of attempts (IQR; 46–86%) compared to 34% of attempts (IQR;

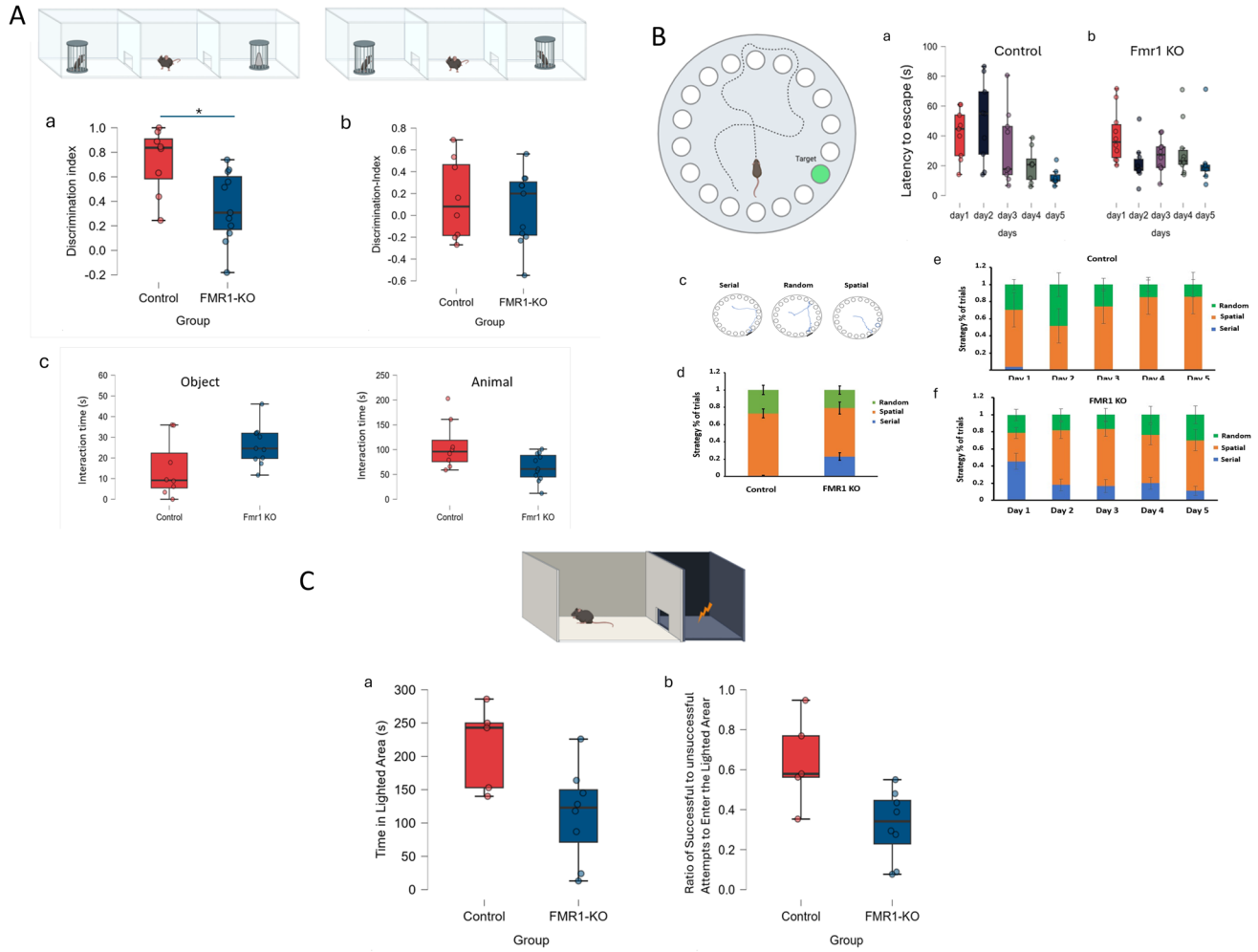

Fig. 1. FMR-KO rats display behavioral phenotypes consistent with ASD. In a sociability task (**A**), the FMR-KO rats show significantly less preference for interacting with another rat, rather than an inanimate object, than controls (a). However, neither the FMR-KO or the control rats display a preference for a novel rat over a familiar one (b). The absolute times spent with the object, or the animal are shown in (c). The Barnes maze (**B**) tests spatial learning over days. The controls show an expected improvement in finding an escape hole over the course of 5 days (a). The FMR-KO rats have a significantly different trajectory over time such that they do not make progress after day 2 (b). The animals' strategy was defined as serial, random or spatial (c) and the proportion of trials per strategy, averaged over the days, is shown in (d). The change in strategy over days in controls is shown in (e) and in FMR-KO rats in (f). The FMR-KO rats also display an anxiety phenotype (**C**) They spend less time in the lit component in the light dark box (a) and are less likely to enter the lit area after poking out their nose than control rats (**b**\). The box plots show the medians inside the box containing the interquartile ranges. The whiskers show the range between the 5th and 95th percentiles.

14–47%) in FMR-KO rats (Wald Chi-Square = 9.8; $p = 0.016$). Thus, both analyses support the view that FMR-KO rats are more anxious than controls.

Neural dynamics

We investigated patterns of action potential firing by recording extracellular single units simultaneously from the hippocampus and the PFC during exploration in an open field. There were no differences in the time in the center, speed or distance travelled between the groups (Fig. 2A). A total of 114 hippocampal pyramidal neurons (58 in controls and 56 in FMR-KO) and 127 PFC neurons (64 in controls and 63 in FMR-KO) in 15 rats (8 control and 7 FMR-KO) were recorded (See Table 1 for details). There were no differences between the groups in terms of firing rate, median interspike interval or action potential half width in either the hippocampus or the PFC (See Table 2).

Action potential firing patterns are abnormal in hippocampus and PFC in FMR-KO rats

Post-spike filters[35–37] were used to evaluate temporal modulation of neuronal firing and estimate patterns of action potential firing over the millisecond (ms) timescale. These filters describe the propensity of a neuron to

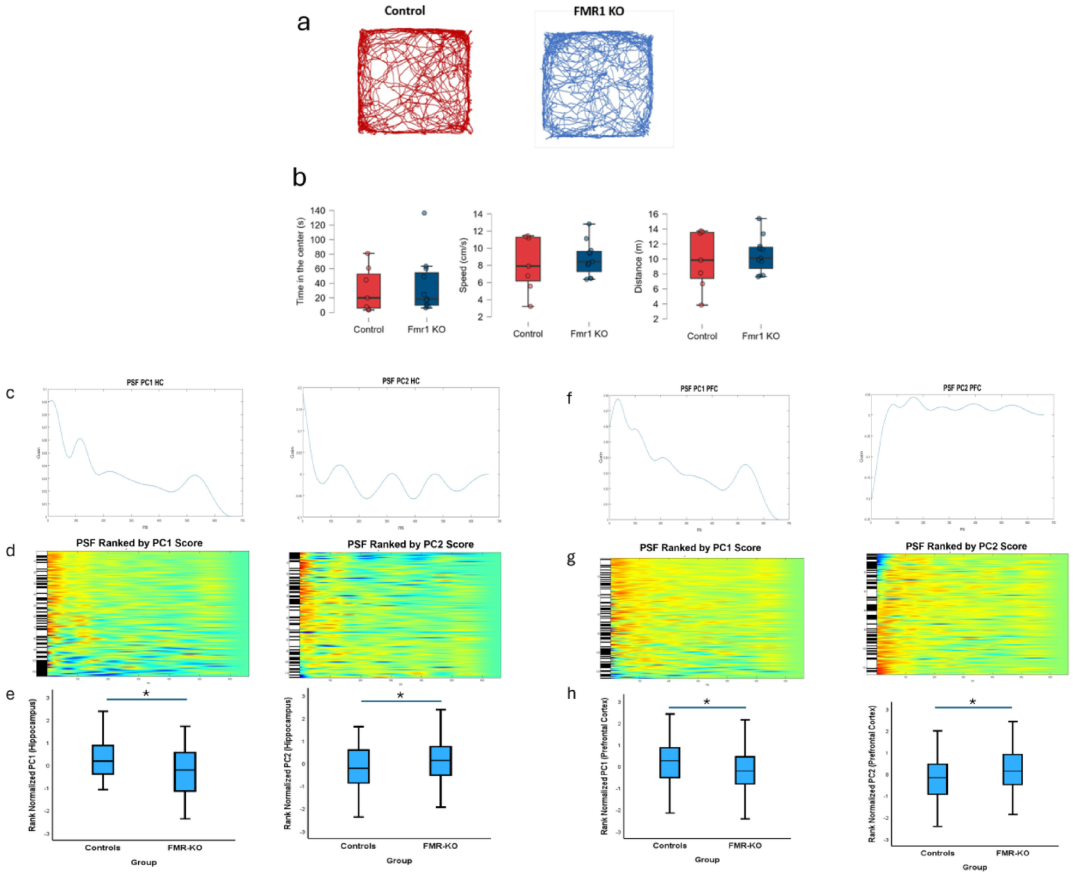

Fig. 2. FMR-KO rats have abnormal action potential dynamics in the hippocampal-PFC circuit. The action potentials were recorded during exploration in an open field. (**a**) shows example tracking plots of a control and FMR-KO rat. The behavior is quantified in (**b**). Hippocampal dynamics are shown in (**c**–**e**), and PFC dynamics are shown in (**f**–**h**). The first 2 principal components (PC) defining the shapes that account for the majority of variance in firing in the hippocampus are shown in (**c**). The first PC from hippocampal recordings shows the neurons have an increased propensity to firing immediately after they have just fired, followed by another increased propensity about 120 ms later (theta modulation, consistent with the expectation for hippocampal neurons). The second PC from the hippocampus reveals an increased propensity to immediate firing following an initial spike with little modulation subsequently (line fluctuates around a gain of zero). In the PFC (**f**), the first PC reveals a propensity to fire about 30 ms after previously firing, with a slow decay in that probability over time. The second PC is dominated by a prolonged refractory period immediately after firing. These two PCs suggest a regular firing pattern, consistent with expected behavior of PFC neurons. The heat maps below the PCs (d and g) show the raw post spike filters ranked in order of PC score. The black marks to the let of the heat maps show the PSFs from FMR-KO animals. The box plots (**f** and **h**) are the quantification of PC scores showing that FMR-KO rats have less theta modulation and increased propensity to fire immediately after firing in the hippocampus, and less robust regular firing in the PFC. The box plots show the medians inside the box containing the interquartile ranges. The whiskers show the range between the 5th and 95th percentiles.

fire over the next 700 ms, given that it has just fired. The filters are quantified using a principal components (PC) analysis and the PC scores are then compared between groups.

In the hippocampus (Fig. 2), the first principal component (PC1) accounted for 57% of the variance and the second principal component (PC2) accounted for 9% of the variance. PC1 captured bursting activity that is typical of hippocampal pyramidal cells. The neurons have a propensity of firing soon after they have previously fired, with subsequent increased propensity to fire about 120 ms later; a burst firing pattern that is modulated in theta. The PC1 score reflects how close the pattern of firing of a neuron is to that canonical pattern. The mean rank normalized[36] PC1 score in the controls was 0.22 ± 0.1 in the controls and -0.23 ± 0.1 in the FMR-KO rats ($F = 26.2$, $df1 = 1$, $df2 = 48$; $p < 0.001$). PC2 mostly captured an immediate increase in firing propensity followed by oscillatory behavior around a gain of zero. The mean rank normalized PC2 score in the controls was -0.29 ± 0.09 and 0.16 ± 0.1 in the FMR-KO rats ($F = 11.9$, $df1 = 1$, $df2 = 47$; $p < 0.001$). Therefore, FMR-KO hippocampal neurons have excessive early bursting behavior and less theta modulation than in controls.

In the PFC (Fig. 2), PC1 accounted for 57% of the variance and PC2 accounted for 13% of the variance. PC1 captures a pattern with most firing occurring approximately 30 ms after a previous spike, with a subsequent smooth decay in firing propensity for the next 700 ms. The mean rank normalized PC1 in the PFC is 0.19 ± 0.1

ID	Number of neurons (Hippocampus)	Number of neurons (PFC)
1	24	6
2	4	1
3	6	13
4	5	10
5	4	6
6	10	14
7	4	14
8	1	0
9	4	1
10	0	6
11	18	4
12	12	18
13	14	6
14	1	6
15	7	22

Table 1. The number of neurons recorded in individual animals. The controls are shown in blue.

	Brain region	Group	Mean	Standard error	*p*-value
Firing rate (Hz)	Hippocampus	Control	0.86	0.20	0.73
		FMR-KO	0.96	0.24	
	PFC	Control	0.81	0.26	0.86
		FMR-KO	0.74	0.30	
Median interspike interval (ms)	Hippocampus	Control	1.24	0.14	0.38
		FMR-KO	1.06	0.15	
	PFC	Control	1.27	0.22	0.31
		FMR-KO	1.63	0.30	
Action potential half width (ms)	Hippocampus	Control	1.8×10^{-4}	4.8×10^{-6}	0.24
		FMR-KO	1.9×10^{-4}	5.3×10^{-6}	
	PFC	Control	1.7×10^{-4}	4.6×10^{-6}	0.96
		FMR-KO	1.7×10^{-4}	1.0×10^{-5}	

Table 2. Action potential firing characteristics in both the hippocampus and the prefrontal cortex in both control and FMR-KO animals.

in controls and -0.20 ± 0.1 in FMR-KO rats ($F=6.8$, $df1=1$, $df2=44$; $p=0.01$). PC2 captures an immediate reduction in the propensity to fire for about 80 ms followed by a period in which firing could occur at any time. The observation that PFC neurons have the capacity to fire across the entire time captured by the PSF suggests that the PFC has capacity for flexible firing that is combined with the regular firing pattern with action potentials occurring 30 ms apart observed in PC1. The mean rank normalized PC2 was -0.24 ± 0.09 in the controls and 0.33 ± 0.08 in the FMR-KO rats ($F=20.4$, $df1=1$, $df2=44$; $p=0.001$). Therefore, in FMR-KO rats the PFC neurons are less likely to fire in a regular firing pattern and are more likely to have a prolonged refractory period than in control rats.

Network structure based on action potential firing patterns are abnormal in FMR-KO rats

We next constructed graphs in which each node in the network is a neuron and the edges are weighted by the dot product between PSF pairs and normalized to the number of total nodes in the network. This generates a fully connected, normalized, weighted, undirected graph describing the synchrogenicity of the network for each session. Synchrogenicity is defined as the similarity in firing patterns of 2 neurons, assuming they received synchronous inputs[37].

The weighted degree is the sum of weights of the edges from each node and is a measure of the density of network connections (Fig. 3). The mean rank normalized weighted degree in controls was 0.42 ± 0.8 and in FMR-KO rats -0.39 ± 0.8 ($F=3.4$, $df1=1$, $df2=236$; $p<0.001$), after adjusting for whether the neuron was recorded from the hippocampus or the PFC. This suggests that networks in control animals are more able to generate synchronous and similar patterns of activity than the FMR-KO rats. The clustering coefficient is a measure of how connected a neuron is to its neighbors and is a measure of network resiliency. A high clustering coefficient indicates that nodes are tightly connected to form a community structure. The mean rank normalized clustering coefficient in controls was 0.36 ± 0.08 and -0.32 ± 0.08 in FMR-KO animals ($p<0.001$, Fig. 3), suggesting that control networks are more resilient to random perturbations than those in FMR-KO rats. There was also a

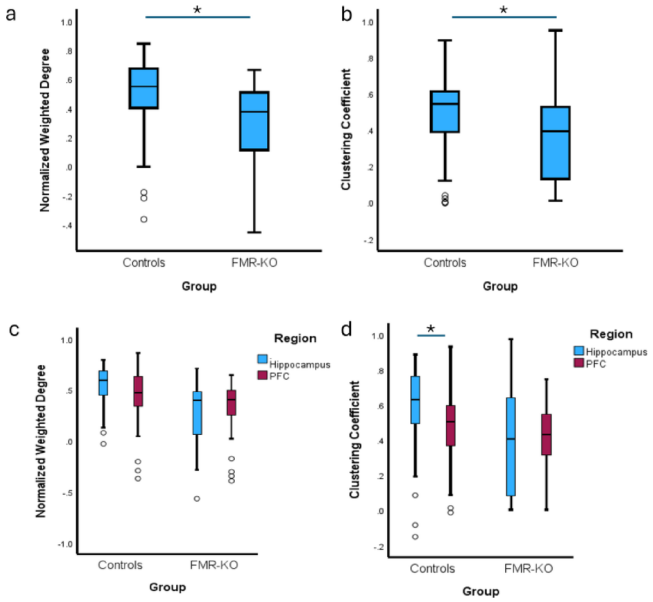

Fig. 3. FMR-KO rats have less organized firing in the hippocampus and less flexible firing in the PFC. The weighted degree (**a**) provides information on the similarities of patterns of firing between neurons in the same animal. There is less similarity in firing patterns in the FMR-KO rats when all neurons are considered. The clustering coefficient (**b**) is a measure of the resiliency of the firing patterns. The FMR-KO animals have lower resiliency than controls. In this circumstance there is a difference in resiliency between the hippocampus and PFC in controls but not in FMR-KO rats. There is no difference between hippocampal similarity and PFC similarity in either the FMR-KO rats or the controls in terms of weighted degree (**c**), but there is a increased hippocampal clustering coefficient when compared to PFC in the controls (**d**). This difference is not seen in the FMR-KO rats.

significant Group*Region interaction ($F = 18.6$, $df1 = 3$, $df2 = 236$; $p = 0.007$). In FMR-KO the mean difference in rank normalized clustering coefficient between the hippocampus and the PFC was 0.1 ± 0.16 ($p = 0.52$) showing that there is similar, albeit low, resiliency across brain structures. In controls the mean difference in rank normalized clustering coefficient was -0.5 ± 0.16 ($p = 0.001$), with the clustering coefficient being lower in the PFC.

There are fewer significant cross-correlations in FMR-KO

We next used cross-correlations to evaluate significant functional relationships in time. For each pair of neurons, we compared the proportion of significantly comodulated neuron pairs between groups in hippocampal-hippocampal, PFC-PFC and hippocampal-PFC pairs (Fig. 4). Control animals were 6.2 times (95% CI 4.5–8.7) more likely to have significant comodulation between pairs of hippocampal neurons than FMR-KO rats (Wald Chi-Square = 133.1, df = 1; $p < 0.001$). For PFC-PFC pairs the controls were 1.8 times (1.3–2.5) times more likely to have significant comodulation than the FMR-KO pairs ($p < 0.001$), and for hippocampus-PFC pairs the controls were 5.4 times (3.9–7.5) more likely to have significant comodulation than FMR-KO pairs ($p < 0.001$). There is also a significant Group*Region interaction ($p < 0.001$). In controls, the hippocampal-hippocampal pairs are most likely to have significant comodulation with the proportion of comodulated pairs being similar for hippocampus-PFC and PFC-PFC. In contrast, in the FMR-KO the proportion of hippocampus-hippocampus and PFC-PFC pairs is similar (albeit lower than in controls) with a very low proportion of hippocampal-PFC pairs being comodulated.

Coupling filters reveal alterations in firing patterns between neuronal pairs

The cross-correlation analysis generated a binary outcome with no information about the patterns of correlated firing of neurons. We therefore built coupling filters that describe the pattern of action potential firing in a neuron, given that another neuron has just fired. The coupling filters were categorized into 4 groups: hippocampal to hippocampal, PFC to PFC, hippocampal to PFC, and PFC to hippocampal neurons. To characterize the similarity in patterns of interactions between neurons we calculated the dot products between coupling filters (Fig. 5). This generated a total of 634,063 dot products in controls and 812,685 dot products in FMR-KO animals. There is no difference between the groups when all the dot products were compared ($p = 0.76$). We then separated the data into dot products from hippocampal to hippocampal, PFC to PFC and hippocampus to PFC filters. The patterns of action potential firing as a function of other neurons firing in the hippocampus are more similar in controls than in FMR-KO animals ($p = 8.8 \times 10^{-9}$). Conversely in both the PFC to PFC ($p = 0.0008$) and hippocampus to PFC ($p = 3.3 \times 10^{-13}$) coupling filters the patterns of firing are less similar in controls when compared to FMR-KO animals.

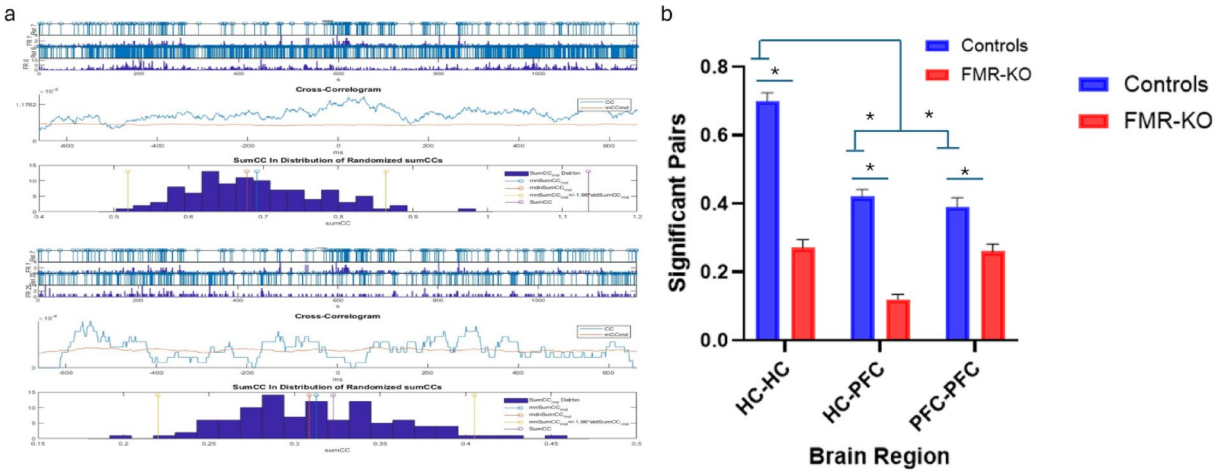

Fig. 4. FMR-KO rats have less coordinated firing in populations of neurons. Panel (**a**) shows examples from 2 pairs of neurons, 1 pair that is not comdulated (top panel) and 1 pair that is comodulated (bottom panel). Each panel shows raster plots from 2 neurons followed by the observed cross-correlogram. The sum of all the values in the actual cross correlogram is then compared to the sum of all values from 100 randomized raster plots (histogram represents the null distribution). The mean, median and 95% confidence intervals are shown on the null distribution. In the top plot, the observed sum is very far outside the upper 95% confidence interval of the null distribution, representing comodulation. In the second example the observed sum is close to the mean of the null distribution, representing lack of comodulation. (**b**) The proportion of comodulated pairs is shown for hippocampal-to-hippocampal, hippocampal to-PFC and PFC-to-PFC pairs in controls and FMR-KO rats. The height of the bar is the mean proportion of significant pairs, and the errors bars represent 1standard error. In all circumstances that comodulation is significantly less in FMR-KO animals. There is also a different pattern of comodulation. In controls the most comodulation was observed in the hippocampus with similar comodulation in HC-PFC and PFC-PFC pairs. In the FMR-KO animals there was similar comodulation in HC-HC and PFC-PFC pairs, with a reduction in comodulation of HC-PFC pairs.

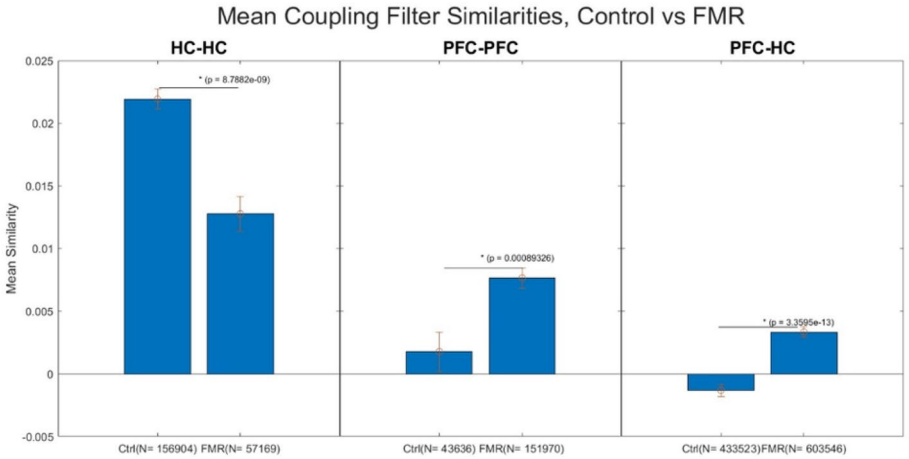

Fig. 5. FMR-KO rats have abnormal patterns of comodulation. In controls the patterns of comodulation are more similar than that observed in FMR-KO rats. However, in hippocampal-to- PFC and in PFC-to-PFC pairs, the patterns of comodulation are less similar in controls than that observed in FMR-KO rats. The height of the bars is the mean similarity score and the bars represent 1 standard error.

Discussion

This study revealed 2 major findings. The first is the confirmation that the FMR-KO rat has behavioral dysfunction across a range of domains[32] including those dependent on H-PFC circuit integrity. The second is that H-PFC circuit action potential dynamics are abnormal in FMR-KO at times that the animal is not participating in the active tasks that it is less able to do. This suggests that loss of Fmr1 protein generates a dysfunctional neural network that is behaving inadequately during exploration and is not able to appropriately engage and support cognition during active tasks. We have previously shown in a model of malformation of cortical development that environmental enrichment recovers both abnormal single unit dynamics during exploration and performance in

the Morris Water Maze[38], supporting the view that therapeutic approaches that recover 'exploring' dynamics in FXS have the potential to prime the network so that it is more able to be engaged in a way that supports active cognitive tasks.

Our behavioral findings are consistent with those previously reported, confirming face validity of the model in our hands. The set of behaviors we tested all have some dependence on the hippocampal-prefrontal cortex circuitry. We recognize that behavioral tasks are never isolated from each other and that the result of any specific test is impacted by cognitive domains that are not specifically being tested e.g. anxiety is likely to have some impact on social behavior and spatial learning in the Barnes maze. However, our goal was not to try and isolate specific behaviors and then to define neural dynamics that underpin the specific behavior. Rather, our goal was to determine whether the spectrum of abnormalities identified in the FMR-KO model are representative of those seen in humans, and then to define abnormal baseline dynamics. We took this approach as strategies that normalize baseline network behavior have enormous potential for recovering *a range* of behaviors rather than attempting to recover behaviors one at a time.

It is known that the formation, organization and maintenance of dendritic spines is abnormal in FMR-KO[39–42]. Dendritic architecture is critically important for receiving inputs into a neuron in a way that allows the information from multiple spines to be integrated within the neuron[43]. The action potential output patterns represent integrated information that is being sent to downstream targets[43]. Inputs arriving at abnormal H-PFC network dendritic spines in FXS are likely to be inadequately integrated with resultant abnormalities in the action potential outputs of the system. Previous studies have identified EEG abnormalities including enhanced gamma power, reduced gamma synchronization and reduced alpha/beta band coherence across frontal, temporal, parietal and occipital brain regions[44–46]. At the level of single units, there is evidence for normal place cell activity, but with abnormal coordination between neuronal firing and phase of the EEG[47]. The current study extends previous studies by explicitly evaluating those output firing patterns of neurons.

Action potential firing dynamics were evaluated in several ways. We started by evaluating firing rate and found that this did not differ between the groups suggesting that it is not firing rate that is critical. We therefore proceeded to evaluate timing and population dynamics.

The initial approach was to establish whether there are abnormalities when neuronal firing is evaluated on a neuron-by-neuron basis. In the hippocampus, neurons typically display burst firing with bursts occurring at theta frequencies[48–50]. Neurons with this behavior are also neurons that effectively encode space and events as determined by the fidelity of place cell firing[51–53]. There were more neurons with this canonical behavior in controls than in FMR-KO animals. In contrast, the PFC is important for executive functions such as attention, behavioral flexibility and decision making, and has been shown to be crucially involved in social behavior and anxiety. These behaviors require a network that is flexible and able to rapidly adapt to sensory inputs. In agreement with this, spontaneous activity of neurons in the PFC is characterized by sporadic firing of weakly correlated pairs of neurons, with some neurons oscillating in delta frequency, punctuated by occasional synchronized activity[54]. The FMR-KO rats have a less canonical firing pattern in the PFC than controls that may underlie the PFC dependent behavioral dysfunctions we observed.

Our next approach was to evaluate whether neurons within animals behaved similarly when they fired. We generated graphs with each neuron as a node and the dot product of the PSFs as edge weights[37], and evaluated two standard graph parameters: the normalized weighted degree and the clustering coefficient. Our control data for weighted degree and clustering coefficients are consistent with prior studies using similar graph-theoretic analyses of hippocampal and parahippocampal structural parameters, fMRI data and modular organization in rats[55,56]. This suggests that normal rodent brain networks, including those involving structurally and specialized regions such as the hippocampus exhibit highly organized connectivity patterns. We show that the FMR-KO animals have less synchronized and less robust patterns of firing than the controls. Thus, the loss of FMR1 protein leads to the emergence of neural networks that are unable to generate robust and similar patterns of action potential firing that support hippocampal-PFC function, and in addition are less able to tolerate any random perturbations that may occur.

There is an interesting difference between network parameters in hippocampus and PFC. In controls there is greater hippocampal firing similarity across neurons and a greater resiliency to random damage than in PFC. This suggests that in the physiological situation there is tightly organized information sent from the hippocampus and that this information is integrated into the PFC in a way that allows flexible outputs, consistent with the requirements for normal executive function. This difference is not observed in the FMR-KO rats with the major reason being that the hippocampus is less resilient. This combination of findings can be interpreted as poorly integrated information in the hippocampus generating inappropriately variable outputs that become poorly integrated inputs to the PFC, negatively impacting flexible firing in the PFC.

We next evaluated how neurons were behaving in time with respect to each other. We initially took a binary approach. We show that FMR-KO animals have far fewer coupled neurons both within structure (i.e. hippocampal-hippocampal and PFC-PFC pairs) and across structures (hippocampal-PFC pairs). This is consistent with previous observations that there are abnormalities in neural communication between the hippocampus and the PFC in ASD[6,57]. The dynamical patterns defined by coupling filters showed more similarity in hippocampal-hippocampal couples in controls than FMR-KO, further supporting the view that the normal hippocampus is a highly organized and integrated functional neural network. In contrast, the similarity in coupled firing in the PFC-PFC couples is lower in controls than in FMR-KO. We posit that this functional organization is appropriate for the PFC as the network receives highly organized information that is integrated in a way that has the network poised to generate short lasting interactions between neurons as the need arises. The more organized firing in the PFC of FMR-KO means that there are less opportunities for flexible functional interactions, and this is likely manifest as more rigid behaviors, consistent with ASD. There is also marked disruption in comodulation of firing across structures with fewer significant couples, but with increased similarity in firing. This suggests

that there is reduced information transfer between hippocampus and PFC, but when there is communication, the information is of poor quality. This further supports the view that abnormal information transfer between the hippocampus and the PFC is important in the pathophysiology of ASD[6,57]. We recognize that functional neural network disruptions in ASD may impact more of the brain than the H-PFC network and that this may be contributing to our results. It is also possible that processes that impact development in children without ASD may also be having a negative effect on the FMR-KO rat H-PFC circuits. However, exploration of those networks will require future studies.

We did not explore whether any of the above patterns correlate with specific active behaviors because the neural dynamics were recorded in one context (exploration) that is unlikely to directly predict behavior in another context, given that those behaviors require different dynamics. It is even more unlikely that dynamics in one context can predict specific performance across a range of tasks. This is akin to the idea that abnormalities in the default mode network[58,59], dorsal attention network[60,61], frontoparietal control network[62] and the cingulo-opercular network[63] all predict that people with Alzheimer's disease will perform poorly in behavioral tasks without predicting specific scores on specific tests. In experimental models, the fidelity of hippocampal CA1 place cell firing predicts that animals will perform poorly is spatial tasks without precise prediction of performance scores[38]. This suggests that there is a 'baseline' functional architecture of neural networks, and the integrity of that network is important for the emergence of specific action potential firing patterns during tasks. We acknowledge that we have not shown a direct relationship between baseline dynamics and engagement of the network during active tasks in this study. However, we have previously shown that environmental enrichment normalizes 'baseline' firing in a model of malformation of cortical development and this is associated with improved spatial cognition. Future studies will attempt to normalize baseline firing with direct manipulation of the H-PFC network to evaluate whether behavior improves, thereby providing a direct link between 'baseline' firing and engagement[38].

In summary, the FMR-KO rat displays several behavioral changes that are consistent with changes identified in autistic people. At the level of the neural network, the inputs to the hippocampal-PFC network are disrupted given the previously identified abnormalities at dendritic spines. This generates a functional network that is less organized, less integrated, and less resilient than expected in controls. This raises the hypothesis that 'exploring' abnormalities are potential therapeutic targets for brain stimulation in which inputs are modified in a way that normalizes those dynamical abnormalities, modifying synaptic weights as a function of activity dependent plasticity which is turn could normalize behavior. Ultimately, such targeted brain stimulation could help to maximize cognitive function in people with FXS that desire such impacts.

Materials and methods

Animals

All animal work was approved by the Nemours Foundation Institutional Animal Care and Use Committee in accordance with the National Institutes of Health Guide for the Care and Use of Laboratory Animals. Male FMR-KO and male control rats were from Envigo Global service Inc Indianapolis, IN. We chose to only use male animals as FXS is predominantly a disorder of males in humans. All animals were housed in the AAALAC-accredited Nemours Children's Hospital Life Science Center. Animals are single housed at a standard 12-h light dark cycle, and water and food were provided ad libitum.

Behavioral experiments

Social interaction:[64] A three-chamber apparatus with a central empty chamber and 2 lateral chambers with a cage where a rat can fit is used. A rat is placed in the empty apparatus for 10 min to explore and then the doors are closed between the chambers. The test animal is put in the central chamber for 3 min while a new rat is put under a cage in one lateral chamber and an inanimate object is placed in the other. The doors are opened for 10 min, and the time spent interacting with the rat in the cage, or the inanimate object, is measured. The doors were closed again for three minutes with the test rat in the central chamber. A second rat is put under the cage in the lateral chamber previously housing the inanimate object. The doors are reopened for 10 min, and the time spent by the test rat interacting with the new and familiar rat in the lateral chambers was measured. A discrimination index was calculated from these times.

Barnes maze:[65] The apparatus is an elevated circular platform (122 cm diameter) with circular holes (10 cm diameter) placed at the edge of the platform. A dark recessed chamber is placed under one of the holes. Pretest: Extra-maze clues are placed in a constant position during the test. The animal is placed at the center of the maze and kept in the dark using a box for 10 s and then the cover is removed, and the animal is guided gently to the dark recessed chamber and allowed to stay for 1 min. Test: the animal is placed under a box in the center of the maze for 10 s and then allowed to search for the hole with the dark recessed chamber. The process is repeated twice at 1-h intervals for 5 days. The test is videotaped for post experiment analysis. The time spent to escape into the chamber was measured. If the animal cannot find the correct hole after 3 min, it is gently guided to it.

Light box/dark box:[33,34] This is a two-compartment paradigm that tests for light anxiety. There is a large light compartment (2/3 of the box is bright and open) and a small dark compartment (1/3 of the box). The compartments are connected by a door that allows the animal to explore freely within the two compartments. The time spent in each compartment is recorded in addition to the number of times the animal put his head outside the dark compartment and the number of times the animal enters the lit compartment immediately following a nose poke. Animals with anxiety are less likely to spend time in, and are less likely to enter, the lit area of the box.

Electrophysiology recordings

Recordings were carried out as previously reported[66]. At P45 rats were anesthetized with isoflurane (2–3% in oxygen) and placed in a stereotaxic frame (Kopf Instruments, Tujunga, CA). Custom-built electrodes were implanted using atlas coordinates into dorsal CA1 of right sided hippocampus and right sided medial PFC (mPFC)[36,66]. Four drivable tetrodes were placed in the hippocampus (coordinates: − 3.2 mm A/P, + 2.2 mm M/L, and 1.7 mm D/V) and two drivable tetrodes in the mPFC (coordinates: + 2.5 mm A/P, + 0.5 mm M/L, − 2.5 mm D/V).

Tetrode assemblies were advanced until CA1 and PFC single-unit activity was detectable. All recordings were carried out during exploration in an open field. The signal from the electrodes was preamplified at the rat's head and transmitted to Neuralynx recording system (Neuralynx, Bozeman, MT). Putative single-unit firing was identified by clustering action potentials from the filtered (500–9000 Hz) signal and thresholded (> 3 × root mean square (RMS) noise) using Neuralynx Spike Sort 3D (Neuralynx, Bozeman, MT). Clusters were evaluated for quality using L-ratio and isolation distance in Spike Sort3D.

Generation of post-spike filters

A post-spike filter is a mathematical function that is proportional to the probability density that a single unit will fire an action potential ("spike") as a function of time after it has fired a previous spike[36]. It is obtained from the observed spike train by finding the probability density that maximizes the likelihood that such a spike train would occur. The probability density is written as a set of basis functions and the coefficients of these basis functions are then be found by numerically maximizing this expression. For the basis functions we used the raised cosine bumps of Pillow and collaborators[35]. To increase goodness of fit we applied penalized regression[35] using Matlab on a Windows-based personal computer. Post-spike filters were made to a maximum time bin of 662 ms.

While more basic and direct statistical measures such as the interspike interval histogram and the autocorrelogram (AC) can give a general idea about this dependence, both are noisy measures which depend on the amount of data collected (firing rate) for the single unit. While the PSF also depends on the amount of data collected, which sets a cutoff firing rate of 0.1 Hz for acceptance in our model, the PSF generally gives a better and smoother model, generally showing good qualitative agreement with the AC, even in cases where the AC struggles to give an interpretable result (See supplementary data).

Generation of coupling filters

The coupling filter of a single unit A influencing the firing of another single unit B is the probability density that B fires a spike as a function of time after A fires a spike. It can be found from the data in a very similar way as for the post-spike filter, but here the spike trains of both single units are used. To do this we used a 32-core cluster running Octave. Similarly, to the post-spike filters, these coupling filters were made to a maximum time bin of 662 ms for forward time only.

Principal component analysis of post-spike and coupling filters

All filters were normalized so that the area under each filter was equal to 1. The post-spike filters were grouped into those recorded from the PFC and those from the hippocampus. The coupling filters were grouped into 4 pools: (1) both from the HC, (2) both from the PFC, (3) target from the HC and source from the PFC, or (4) target from the PFC and source from the HC. Using Matlab, uncentered Principal Component (PC) Analysis was performed on each pool separately. The mean normalized filter for each group was plotted side by side in a heat map, sorted by PC1 and PC2 scores, respectively.

Similarity analysis of post-spike filters and coupling filters

Within each ensemble of single units from each recording session, the similarity of each filter to every other filter was quantified by first normalizing and then taking the dot product of each filter to every other filter. For each pair of normalized filters, the result will be a number between 1 for filters which are identical, and -1 for filters which are the negatives of each other.

Pairwise analyses

To identify significant interactions between neurons we computed the cross-correlogram from a time lag of − 662 ms to a time lag of 662 ms. We then compared the observed cross-correlogram to a statistical ensemble of 100 randomized cross-correlograms made by shifting the raster of one cluster relative to the other. This shift was made by randomly cutting the raster and appending the second section to the beginning section. Thus, rasters are randomized with respect to one another, while preserving mean firing rate, mean, median and standard deviation of the interspike interval, and autocorrelogram of each raster. The sum of all the values of the randomized cross-correlograms followed an approximately normal distribution. If the sum of the actual cross-correlogram of the two neurons was above the 95% confidence interval of the randomized cross-correlograms, then the actual cross-correlogram was determined to be significant.

Statistical analyses

A variety of approaches were used, depending on the type of analysis. For the analyses of sociability each session was considered separately and differences between groups were evaluated using a Mann–Whitney U. The same test was used for the 2 analyses for light–dark box. In all other circumstances there were multiple observations per animal and therefore we used generalized linear mixed models (GLMM) to ensure appropriate distributions for the data and to account for within-animal correlations as a function of multiple observations. For the Barnes maze the multiple observations were trials over multiple days. For the electrophysiological data the multiple

observations were the number of single units recorded simultaneously. On inspection, the distributions of the principal component scores and similarity scores were frequently difficult to define and therefore we chose to perform an inverse rank-based normal transformation that resulted in a normal distribution with a mean of zero and a standard deviation of one. This is a conservative approach as the magnitude of difference is lost by ranking. Binary pairwise data was analyzed with a binary logistic approach within the GLMM framework.

Data availability

All data will be available by request to the corresponding author.

Received: 9 January 2025; Accepted: 21 April 2025
Published online: 08 May 2025

References

1. Belmonte, M. K. & Bourgeron, T. Fragile X syndrome and autism at the intersection of genetic and neural networks. *Nat. Neurosci.* **9** (10), 1221–1225. https://doi.org/10.1038/nn1765 (2006).
2. Hagerman, R. J. et al. Fragile X syndrome. *Nat. Rev. Dis. Primer*. **3**, 17065. https://doi.org/10.1038/nrdp.2017.65 (2017).
3. Lamanna, J. & Meldolesi, J. Autism spectrum disorder: Brain areas involved, Neurobiological mechanisms, diagnoses and therapies. *Int. J. Mol. Sci.* **25** (4), 2423. https://doi.org/10.3390/ijms25042423 (2024).
4. Majhi, S., Kumar, S. & Singh, L. A review on autism spectrum disorder: Pathogenesis, biomarkers, pharmacological and non-pharmacological interventions. *CNS Neurol. Disord Drug Targets*. **22** (5), 659–677. https://doi.org/10.2174/1871527321666220428134802 (2023).
5. Wang, L., Wang, B., Wu, C., Wang, J. & Sun, M. Autism spectrum disorder: Neurodevelopmental risk factors, biological mechanism, and precision therapy. *Int. J. Mol. Sci.* **24** (3), 1819. https://doi.org/10.3390/ijms24031819 (2023).
6. Banker, S. M., Gu, X., Schiller, D. & Foss-Feig, J. Hippocampal contributions to social and cognitive deficits in autism spectrum disorder. *Trends Neurosci.* **44** (10), 793–807. https://doi.org/10.1016/j.tins.2021.08.005 (2021).
7. Leisman, G., Melillo, R. & Melillo, T. Prefrontal functional connectivities in autism spectrum disorders: A connectopathic disorder affecting movement, interoception, and cognition. *Brain Res. Bull.* **198**, 65–76. https://doi.org/10.1016/j.brainresbull.2023.04.004 (2023).
8. Cunniff, M. M., Markenscoff-Papadimitriou, E., Ostrowski, J., Rubenstein, J. L. R. & Sohal, V. S. Altered hippocampal-prefrontal communication during anxiety-related avoidance in mice deficient for the autism-associated gene Pogz. *eLife* https://doi.org/10.7554/eLife.54835 (2020).
9. Kemper, T. L. & Bauman, M. L. The contribution of neuropathologic studies to the Understanding of autism. *Neurol. Clin.* **11** (1), 175–187 (1993).
10. Raymond, G. V., Bauman, M. L. & Kemper, T. L. Hippocampus in autism: A golgi analysis. *Acta Neuropathol. (Berl).* **91** (1), 117–119. https://doi.org/10.1007/s004010050401 (1995).
11. Eilam-Stock, T., Tingting, W., Spagna, A., Egan, L. J. & Fan, J. Neuroanatomical alterations in high-functioning adults with autism spectrum disorder. *Front. Neurosci.* https://doi.org/10.3389/fnins.2016.00237 (2016).
12. Ameis, S. H. & Szatmari, P. Imaging-genetics in autism spectrum disorder: Advances, translational impact, and future directions. *Front. Psychiatry* https://doi.org/10.3389/fpsyt.2012.00046 (2012).
13. Rinaldi, T. Hyper-connectivity and hyper-plasticity in the medial prefrontal cortex in the valproic acid animal model of autism. *Front. Neural Circuits* https://doi.org/10.3389/neuro.04.004.2008 (2008).
14. Padilla-Coreano, N. et al. Direct ventral Hippocampal-Prefrontal input is required for Anxiety-Related neural activity and behavior. *Neuron* **89** (4), 857–866. https://doi.org/10.1016/j.neuron.2016.01.011 (2016).
15. Hsu, P. J. et al. The RNA-binding protein FMRP facilitates the nuclear export of N6-methyladenosine-containing mRNAs. *J. Biol. Chem.* **294** (52), 19889–19895. https://doi.org/10.1074/jbc.AC119.010078 (2019).
16. Verkerk, A. J. et al. Identification of a gene (FMR-1) containing a CGG repeat coincident with a breakpoint cluster region exhibiting length variation in fragile X syndrome. *Cell* **65** (5), 905–914. https://doi.org/10.1016/0092-8674(91)90397-h (1991).
17. Westmark, C. J., Maloney, B., Alisch, R. S., Sokol, D. K. & Lahiri, D. K. FMRP regulates the nuclear export of Adam9 and Psen1 mRNAs: Secondary analysis of an N6-Methyladenosine dataset. *Sci. Rep.* **10**, 10781. https://doi.org/10.1038/s41598-020-66394-y (2020).
18. Taha, M. S. & Ahmadian, M. R. Fragile X messenger ribonucleoprotein protein and its multifunctionality: From cytosol to nucleolus and back. *Biomolecules* **14** (4), 399. https://doi.org/10.3390/biom14040399 (2024).
19. Willemsen, R. & Kooy, R. F. Mouse models of fragile X-related disorders. *Dis. Model. Mech.* **16** (2), dmm049485. https://doi.org/10.1242/dmm.049485 (2023).
20. Bongmba, O. Y. N., Martinez, L. A., Elhardt, M. E., Butler, K. & Tejada-Simon, M. V. Modulation of dendritic spines and synaptic function by Rac1: A possible link to fragile X syndrome pathology. *Brain Res.* **1399**, 79–95. https://doi.org/10.1016/j.brainres.2011.05.020 (2011).
21. Fu, Y. H. et al. Variation of the CGG repeat at the fragile X site results in genetic instability: Resolution of the Sherman paradox. *Cell* **67** (6), 1047–1058. https://doi.org/10.1016/0092-8674(91)90283-5 (1991).
22. Han, K. et al. Fragile X-like behaviors and abnormal cortical dendritic spines in cytoplasmic FMR1-interacting protein 2-mutant mice. *Hum. Mol. Genet.* **24** (7), 1813–1823. https://doi.org/10.1093/hmg/ddu595 (2015).
23. Lu, R. et al. The fragile X protein controls microtubule-associated protein 1B translation and microtubule stability in brain neuron development. *Proc. Natl. Acad. Sci. U S A.* **101** (42), 15201–15206. https://doi.org/10.1073/pnas.0404995101 (2004).
24. Maurin, T., Zongaro, S., Bardoni, B. & Fragile, X. Syndrome: From molecular pathology to therapy. *Neurosci. Biobehav. Rev.* **46 Pt 2**, 242–255. https://doi.org/10.1016/j.neubiorev.2014.01.006 (2014).
25. Messaoudi, S. et al. FMRP regulates postnatal neuronal migration via MAP1B. *eLife* **12**, RP88782. https://doi.org/10.7554/eLife.88782 (2024).
26. Michaelsen-Preusse, K., Feuge, J. & Korte, M. Imbalance of synaptic actin dynamics as a key to fragile X syndrome? *J. Physiol.* **596** (14), 2773–2782. https://doi.org/10.1113/JP275571 (2018).
27. Pieretti, M. et al. Absence of expression of the FMR-1 gene in fragile X syndrome. *Cell* **66** (4), 817–822. https://doi.org/10.1016/0092-8674(91)90125-i (1991).
28. Sears, J. C. & Broadie, K. Fragile X mental retardation protein regulates activity-dependent membrane trafficking and trans-synaptic signaling mediating synaptic remodeling. *Front. Mol. Neurosci.* https://doi.org/10.3389/fnmol.2017.00440 (2018).
29. Doll, C. A. & Broadie, K. Impaired activity-dependent neural circuit assembly and refinement in autism spectrum disorder genetic models. *Front. Cell. Neurosci.* https://doi.org/10.3389/fncel.2014.00030 (2014).
30. Doll, C. A. & Broadie, K. Activity-dependent FMRP requirements in development of the neural circuitry of learning and memory. *Dev. Camb. Engl.* **142** (7), 1346–1356. https://doi.org/10.1242/dev.117127 (2015).
31. Doll, C. A., Vita, D. J., Broadie, K. & Fragile, X. Mental retardation protein requirements in activity-dependent critical period neural circuit refinement. *Curr. Biol. CB.* **27** (15), 2318–2330e3. https://doi.org/10.1016/j.cub.2017.06.046 (2017).

32. Kat, R. et al. Translational validity and methodological underreporting in animal research: A systematic review and meta-analysis of the fragile X syndrome (Fmr1 KO) rodent model. *Neurosci. Biobehav. Rev.* **139**, 104722. https://doi.org/10.1016/j.neubiorev.2022.104722 (2022).
33. Bourin, M. & Hascoët, M. The mouse light/dark box test. *Eur. J. Pharmacol.* **463** (1–3), 55–65. https://doi.org/10.1016/s0014-2999(03)01274-3 (2003).
34. Takao, K. & Miyakawa, T. Light/dark transition test for mice. *J. Vis. Exp. JoVE.* **1**, 104. https://doi.org/10.3791/104 (2006).
35. Pillow, J. W. et al. Spatio-temporal correlations and visual signalling in a complete neuronal population. *Nature* **454** (7207), 995–999. https://doi.org/10.1038/nature07140 (2008).
36. Hernan, A. E., Matthew Mahoney, J., Curry, W., Mawe, S. & Scott, R. C. Fine spike timing in hippocampal–prefrontal ensembles predicts poor encoding and underlies behavioral performance in healthy and malformed brains. *Cereb. Cortex N Y N 1991* **31**(1), 147–158. https://doi.org/10.1093/cercor/bhaa216 (2021).
37. Chari, A. et al. Single unit-derived connectivity networks in tuberous sclerosis complex reveal propensity for network hypersynchrony driven by tuber-tuber interactions. *Sci. Rep.* **14** (1), 31654. https://doi.org/10.1038/s41598-024-80634-5 (2024).
38. Jenks, K. R. et al. Enrichment and training improve cognition in rats with cortical malformations. *PLoS ONE.* **8** (12), e84492. https://doi.org/10.1371/journal.pone.0084492 (2013).
39. Berman, R. F., Murray, K. D., Arque, G., Hunsaker, M. R. & Wenzel, H. J. Abnormal dendrite and spine morphology in primary visual cortex in the CGG knock-in mouse model of the fragile X premutation. *Epilepsia* **53** (0 1), 150–160. https://doi.org/10.1111/j.1528-1167.2012.03486.x (2012).
40. Grossman, A. W. et al. Developmental characteristics of dendritic spines in the dentate gyrus of Fmr1 knockout mice. *Brain Res.* **1355**, 221–227. https://doi.org/10.1016/j.brainres.2010.07.090 (2010).
41. He, C. X. & Portera-Cailliau, C. The trouble with spines in fragile X syndrome: Density, maturity and plasticity. *Neuroscience* **251**, 120. https://doi.org/10.1016/j.neuroscience.2012.03.049 (2013).
42. McKinney, B. C., Grossman, A. W., Elisseou, N. M. & Greenough, W. T. Dendritic spine abnormalities in the occipital cortex of C57BL/6 Fmr1 knockout mice. *Am. J. Med. Genet. Part. B Neuropsychiatr Genet. Off Publ Int. Soc. Psychiatr Genet.* **136B** (1), 98–102. https://doi.org/10.1002/ajmg.b.30183 (2005).
43. Fischer, L. et al. Dendritic mechanisms for in vivo neural computations and behavior. *J. Neurosci.* **42** (45), 8460–8467. https://doi.org/10.1523/JNEUROSCI.1132-22.2022 (2022).
44. Lovelace, J. W., Ethell, I. M., Binder, D. K. & Razak, K. A. Translation-relevant EEG phenotypes in a mouse model of fragile X syndrome. *Neurobiol. Dis.* **115**, 39–48. https://doi.org/10.1016/j.nbd.2018.03.012 (2018).
45. Lovelace, J. W. et al. Deletion of Fmr1 from forebrain excitatory neurons triggers abnormal cellular, EEG, and behavioral phenotypes in the auditory cortex of a mouse model of fragile X syndrome. *Cereb. Cortex.* **30** (3), 969–988. https://doi.org/10.1093/cercor/bhz141 (2020).
46. Janz, P., Bainier, M., Marashli, S., Gross, S. & Redondo, R. L. Clinically-probed mechanisms of action in Fragile-X syndrome fail to normalize translational EEG phenotypes in Fmr1 knockout mice. *Neuropharmacology* **262**, 110182. https://doi.org/10.1016/j.neuropharm.2024.110182 (2025).
47. Talbot, Z. N. et al. Normal CA1 place fields but discoordinated network discharge in a Fmr1-Null mouse model of fragile X syndrome. *Neuron* **97** (3), 684–697e4. https://doi.org/10.1016/j.neuron.2017.12.043 (2018).
48. Harris, K. D. et al. Spike train dynamics predicts theta-related phase precession in hippocampal pyramidal cells. *Nature* **417** (6890), 738–741. https://doi.org/10.1038/nature00808 (2002).
49. Hirase, H., Czurkó, A., Csicsvari, J. & Buzsáki, G. Firing rate and theta-phase coding by hippocampal pyramidal neurons during space clamping. *Eur. J. Neurosci.* **11** (12), 4373–4380. https://doi.org/10.1046/j.1460-9568.1999.00853.x (1999).
50. Mizuseki, K., Diba, K., Pastalkova, E. & Buzsáki, G. Hippocampal CA1 pyramidal cells form functionally distinct sublayers. *Nat. Neurosci.* **14** (9), 1174–1181. https://doi.org/10.1038/nn.2894 (2011).
51. Harvey, C. D., Collman, F., Dombeck, D. A. & Tank, D. W. Intracellular dynamics of hippocampal place cells during virtual navigation. *Nature* **461** (7266), 941–946. https://doi.org/10.1038/nature08499 (2009).
52. Jeewajee, A. et al. Theta phase precession of grid and place cell firing in open environments. *Philos. Trans. R. Soc. B Biol. Sci.* **369** (1635), 20120532. https://doi.org/10.1098/rstb.2012.0532 (2014).
53. Royer, S. et al. Control of timing, rate and bursts of hippocampal place cells by dendritic and somatic inhibition. *Nat. Neurosci.* **15** (5), 769–775. https://doi.org/10.1038/nn.3077 (2012).
54. Blaeser, A. S., Connors, B. W. & Nurmikko, A. V. Spontaneous dynamics of neural networks in deep layers of prefrontal cortex. *J. Neurophysiol.* **117** (4), 1581–1594. https://doi.org/10.1152/jn.00295.2016 (2017).
55. Binicewicz, F. Z. M., van Strien, N. M., Wadman, W. J., van den Heuvel, M. P. & Cappaert, N. L. M. Graph analysis of the anatomical network organization of the hippocampal formation and parahippocampal region in the rat. *Brain Struct. Funct.* **221** (3), 1607–1621. https://doi.org/10.1007/s00429-015-0992-0 (2016).
56. Fardet, T. & Levina, A. Weighted directed clustering: Interpretations and requirements for heterogeneous, inferred, and measured networks. *Phys. Rev. Res.* **3** (4), 043124. https://doi.org/10.1103/PhysRevResearch.3.043124 (2021).
57. Long, J. et al. Insights into the structure and function of the hippocampus: Implications for the pathophysiology and treatment of autism spectrum disorder. *Front. Psychiatry.* **15**, 1364858. https://doi.org/10.3389/fpsyt.2024.1364858 (2024).
58. Eyler, L. T. et al. Resting state abnormalities of the default mode network in mild cognitive impairment: A systematic review and Meta-Analysis. *J. Alzheimers Dis. JAD.* **70** (1), 107–120. https://doi.org/10.3233/JAD-180847 (2019).
59. Wang, Y. et al. Shared and differing functional connectivity abnormalities of the default mode network in mild cognitive impairment and Alzheimer's disease. *Cereb. Cortex N Y N 1991.* **34** (3), bhae094. https://doi.org/10.1093/cercor/bhae094 (2024).
60. Franzmeier, N. et al. Resting-state connectivity of the left frontal cortex to the default mode and dorsal attention network supports reserve in mild cognitive impairment. *Front. Aging Neurosci.* **9**, 264. https://doi.org/10.3389/fnagi.2017.00264 (2017).
61. Wu, H. et al. Functional and structural alterations of dorsal attention network in preclinical and early-stage Alzheimer's disease. *CNS Neurosci. Ther.* **29** (6), 1512–1524. https://doi.org/10.1111/cns.14092 (2023).
62. Boyle, R. et al. Left frontoparietal control network connectivity moderates the effect of amyloid on cognitive decline in preclinical Alzheimer's disease: The A4 study. *J. Prev. Alzheimers Dis.* **11** (4), 881–888. https://doi.org/10.14283/jpad.2024.140 (2024).
63. Yang, H. et al. Hypoconnectivity within the cingulo-opercular network in patients with mild cognitive impairment in Chinese communities. *Int. J. Geriatr. Psychiatry.* **38** (8), e5979. https://doi.org/10.1002/gps.5979 (2023).
64. Kim, D. G. et al. Social interaction test in home cage as a novel and ethological measure of social behavior in mice. *Exp. Neurobiol.* **28** (2), 247–260. https://doi.org/10.5607/en.2019.28.2.247 (2019).
65. Pitts, M. W. Barnes maze procedure for spatial learning and memory in mice. *Bio-Protoc.* **8** (5), e2744. https://doi.org/10.21769/BioProtoc.2744 (2018).
66. Lucas, M. M., Lenck-Santini, P. P., Holmes, G. L. & Scott, R. C. Impaired cognition in rats with cortical dysplasia: Additional impact of early-life seizures. *Brain* **134**(Pt 6), 1684–1693. https://doi.org/10.1093/brain/awr087 (2011).

Acknowledgements

This work received funding from the Swank Foundation, R21NS117112 (RS) and start-up funds from the Nemours Foundation.

Author contributions

RS, JM, AH – Experimental design, oversight of experiments, drafting manuscriptMO – experimental design, conduct of experiments, initial signal processingPJ, MK, JM – Data analysis (PSFs, CFs, Cross-correlograms, graph statistics)RS – Statistical analysis.

Declarations

Competing interests

The authors declare no competing interests.

Additional information

Supplementary Information The online version contains supplementary material available at https://doi.org/10.1038/s41598-025-99408-8.

Correspondence and requests for materials should be addressed to R.C.S.

Reprints and permissions information is available at www.nature.com/reprints.

Publisher's note Springer Nature remains neutral with regard to jurisdictional claims in published maps and institutional affiliations.